Supplementary Information

1. Parametric study on the width of BPCM

We conduct a parametric study to determine the influence on the width of BPCM on the CTE and PR of BPCM. The numerical simulation was conducted for 10 randomly selected BPCMs with a variation of width from 1.6 mm to 2.4 mm at 0.2 mm intervals as shown in Fig S1. Such results suggest that the increase in the width of BPCM leads to the gradual increase of the CTE, while the variation in the width of BPCM exhibits negligible influence on PR. Given that other studies investigating the effect of width on chiral structural mechanical metamaterials with arc-shaped ribs suggest a similar correlation between the width and the CTE and PR, such results are considered valid.[1, 2] The results of the parametric study on width suggest that the thinner width of BPCM leads to the achievement of a large amplitude of NTE. However, as an excessively thin width of BPCM may result in quality deterioration of 3D printed BPCM and handle issues during the tensile test due to the weak mechanical properties, the width of BPCM is set to 2mm.

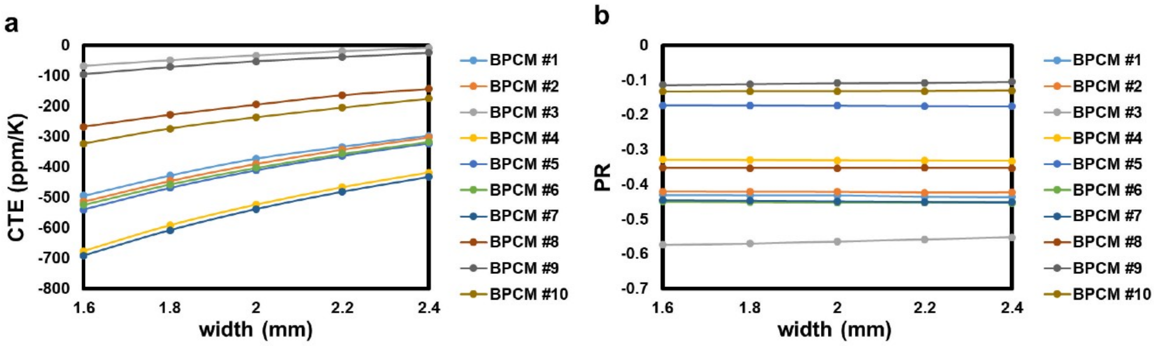

Fig. S1 The CTE and PR of randomly selected BPCM according to the variation of the width

Table S1 Bezier curve control points and numerical simulation results of the randomly selected BPCM with a width of 2mm

	P_{x1}	P_{y1}	P_{x2}	P_{x2}	CTE	PR
BPCM #1	9.99	15.09	3.57	10.31	-372.777	-0.4322
BPCM #2	12.49	16.7	2.19	10.03	-389.891	-0.42197
BPCM #3	0.24	6.91	12.57	1.41	-33.9224	-0.56472
BPCM #4	8.9	18.78	14.97	7.15	-524.243	-0.33167
BPCM #5	4.62	1.25	16.04	19.47	-411.963	-0.17435
BPCM #6	7.05	18.38	9.78	5.11	-402.886	-0.45255
BPCM #7	1.63	13.06	6.42	14.35	-539.07	-0.4485
BPCM #8	17.96	15.75	6.7	1.24	-195.378	-0.35374
BPCM #9	16.46	1.1	6.62	10.75	-53.0355	-0.1094
BPCM #10	13.68	0.07	7.91	18.02	-237.356	-0.13271

2. The numerical simulation results of BPCM configured with other parametric curves

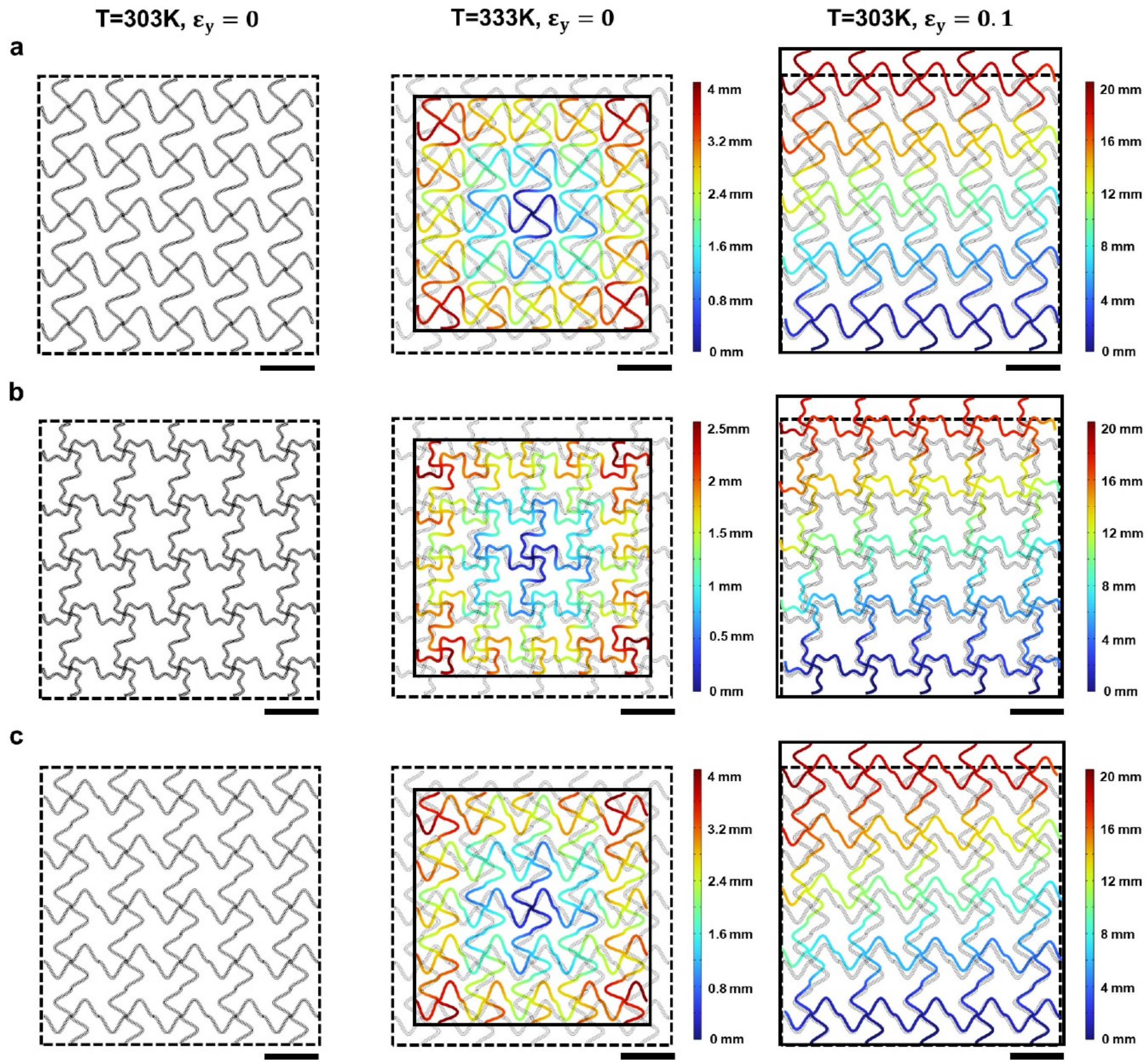

Fig. S2 The numerical simulation results of BPCM configured with other parametric curves, scale factor = 4.5 (a) Polynomial function: $y = -0.01x^2(x-20)$ CTE= -664.37 ppm/k, PR= -0.1548 (b) Polynomial function: $y = -0.002x(x-20)(x^2-20x+120)$ CTE= -444.25 ppm/k, PR= -0.3367 (c) Trigonometric function: $y = -6\cos\left(\frac{\pi x}{10}\right) + 6$ CTE= -629.33 ppm/k, PR= -0.2893 (All scale bars are 40mm)

3. Detailed network structure of DAIM

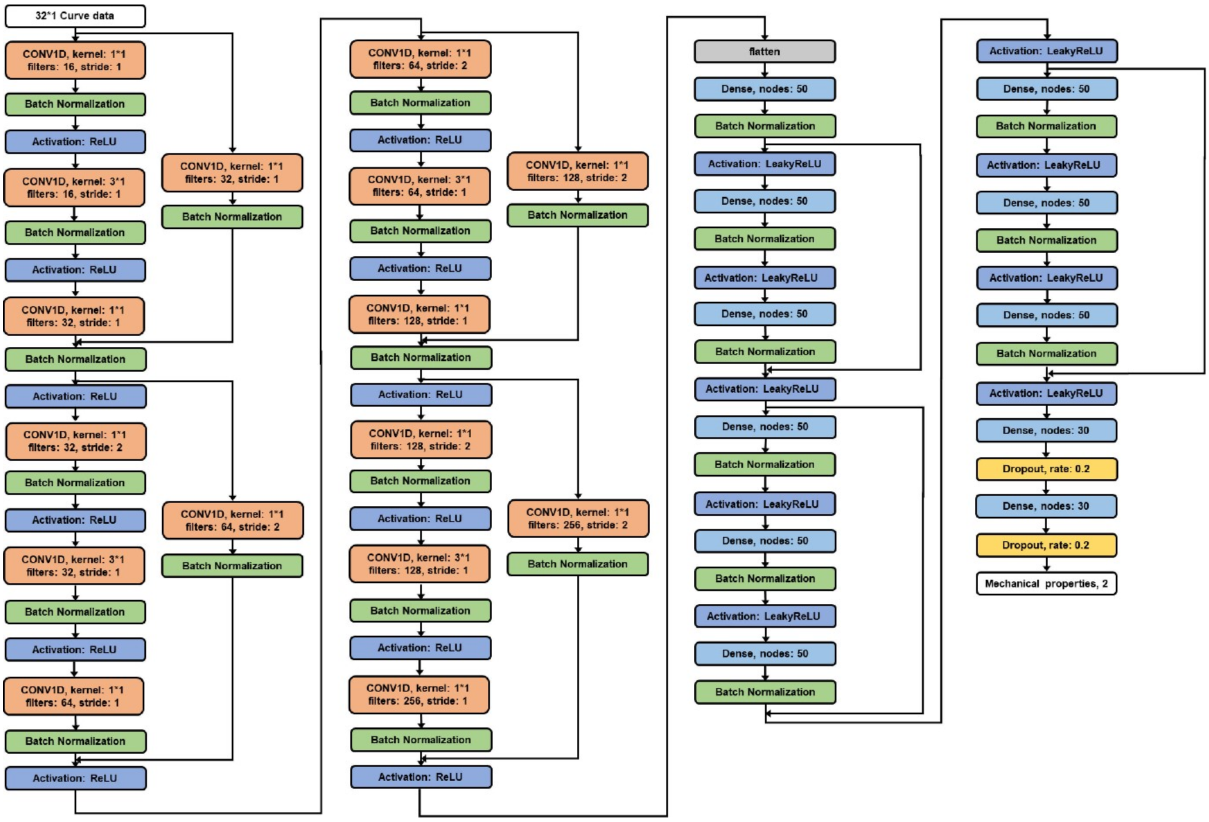

Fig. S3 The neural network structure of the DAIM encoder part (prediction model)

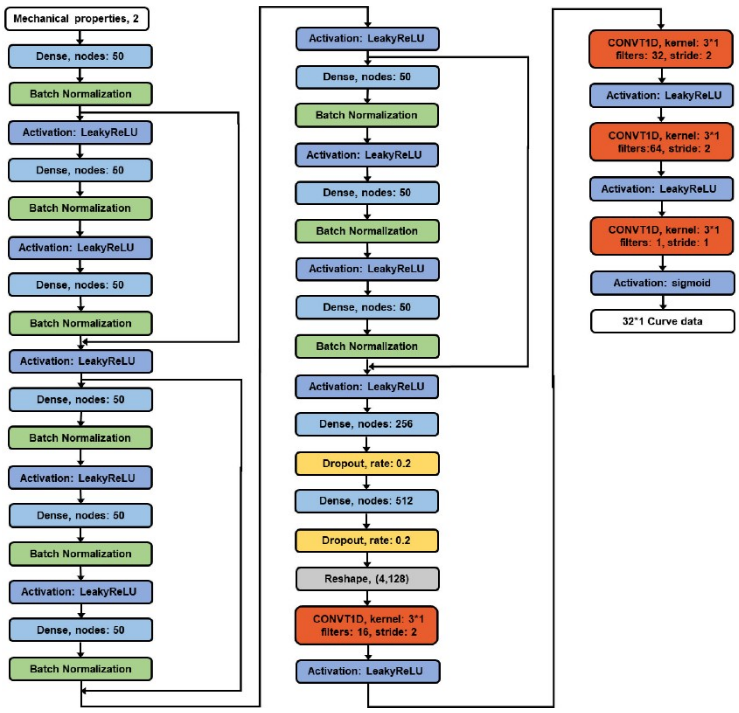

Fig. S4 The neural network structure of the DAIM decoder part (inverse design model)

4. Learning curve of the DAIM

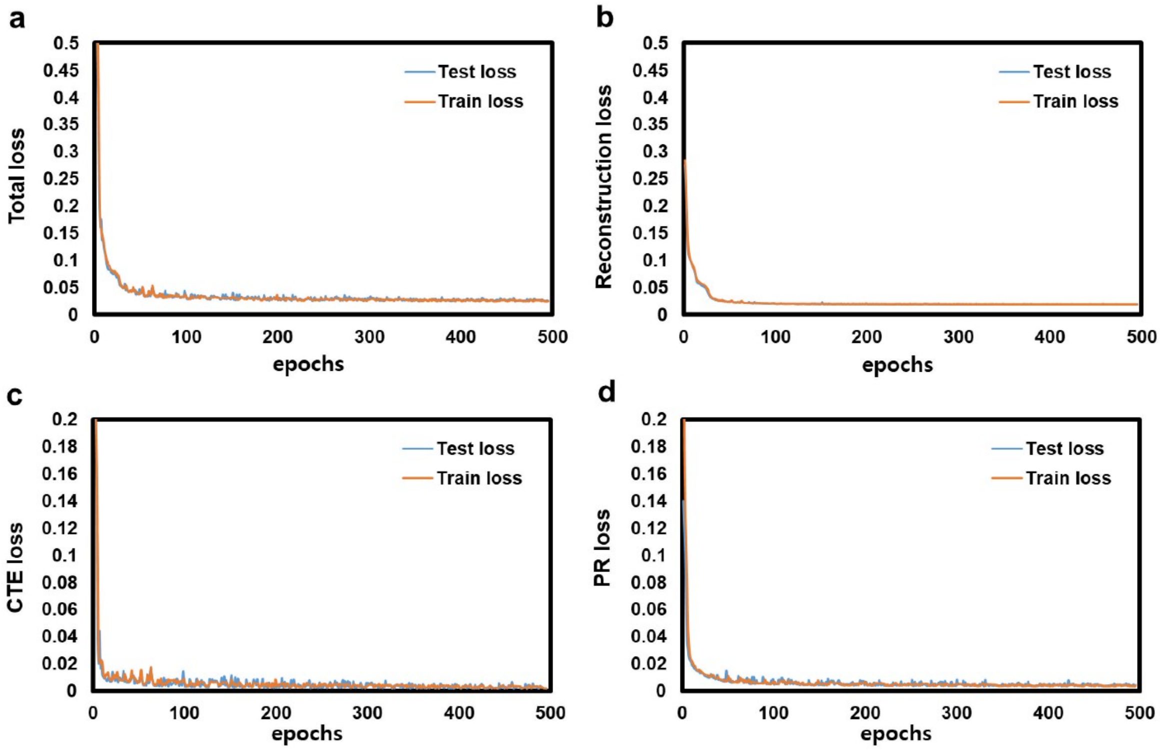

Figs. S5 Learning curve of DAIM (a) total loss (b) reconstruction loss (c) CTE loss (d) PR loss

5. Detailed information about the process of iterative transfer learning

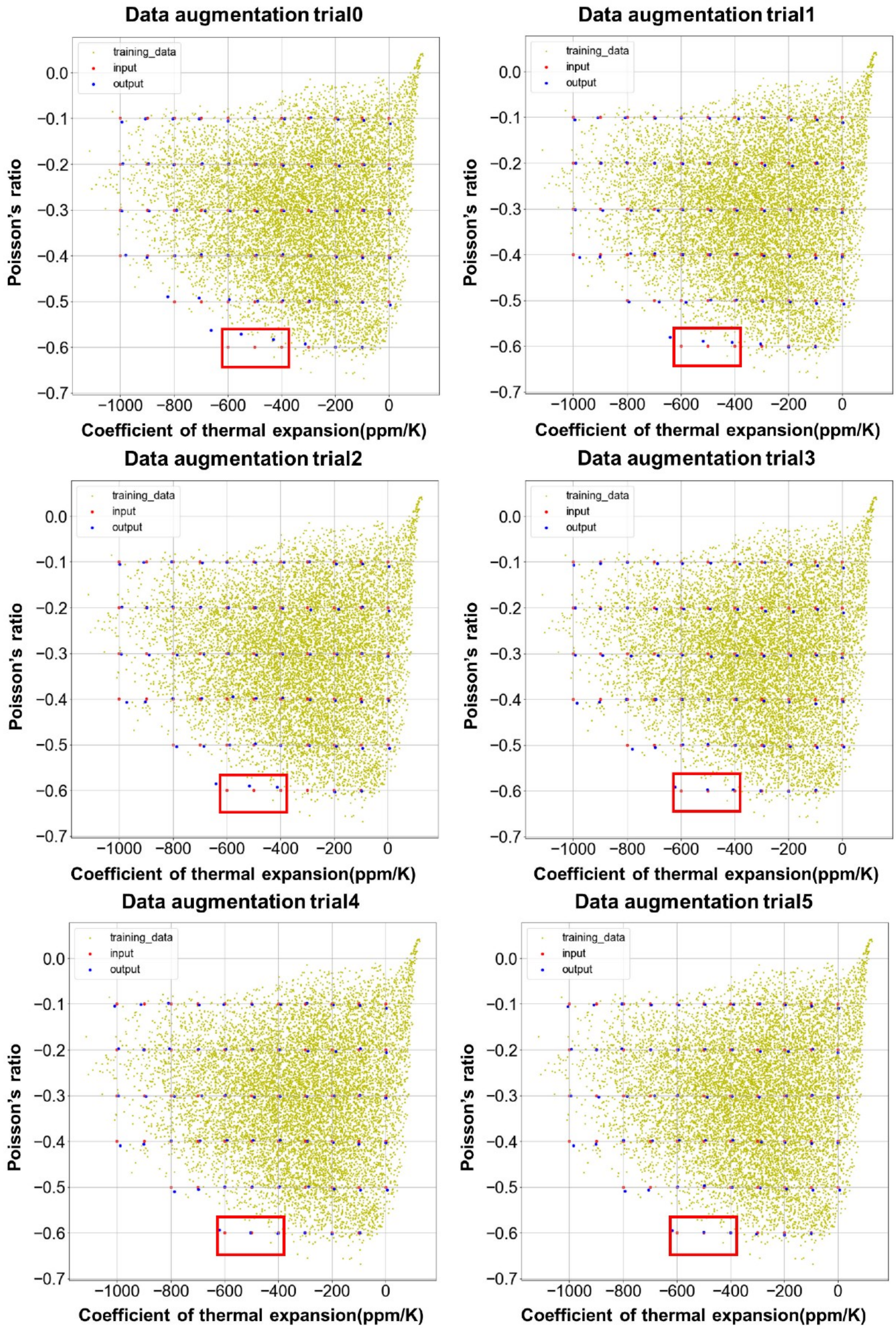

Fig. S6 Inverse design result improvement according to transfer learning with data augmentation iteration for area1

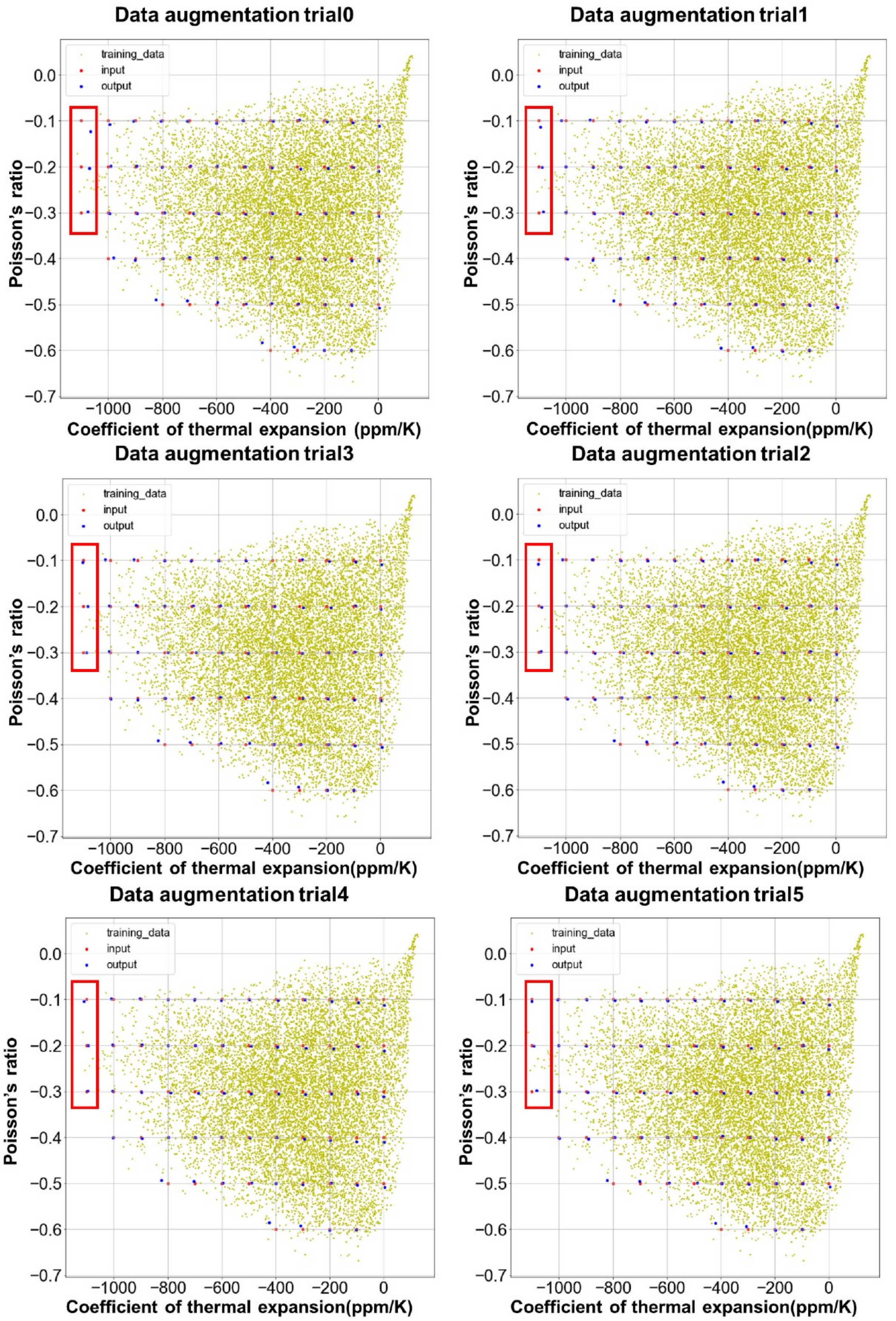

Fig. S7 Inverse design result improvement according to transfer learning with data augmentation iteration for area 2

6. Results of experimental validation

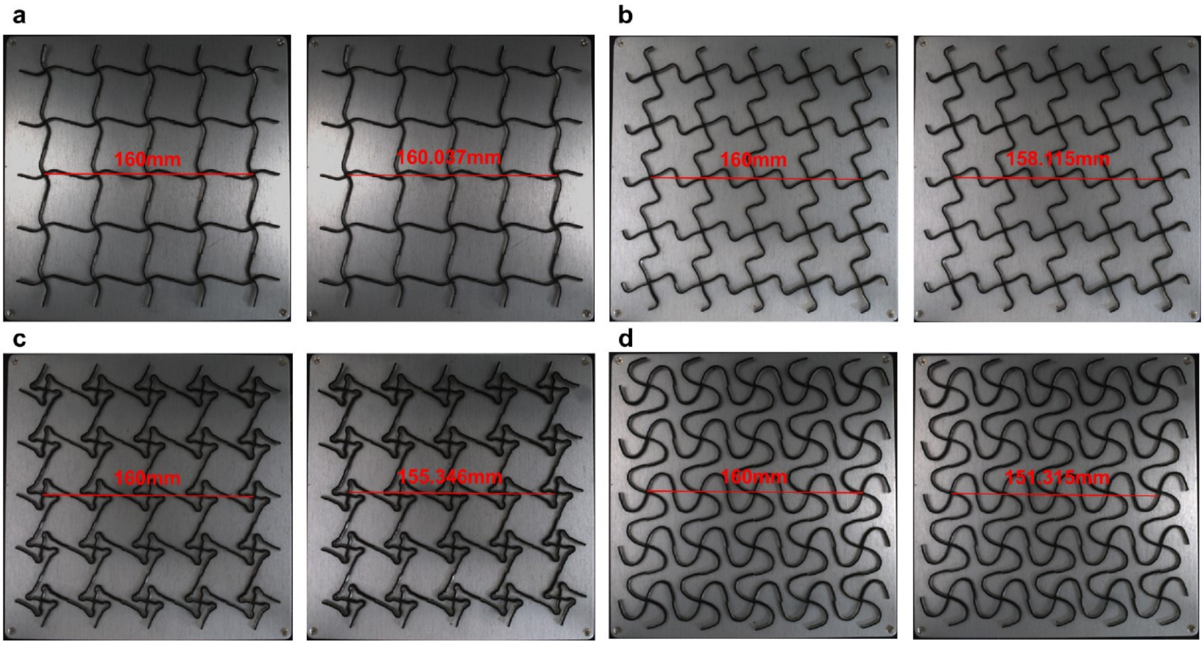

Fig. S8 Thermal expansion experiment result (a) inverse design target CTE = 0 ppm/K (b) inverse design target CTE = -200 ppm/K (c) inverse design target CTE = -500 ppm/K (d) inverse design target CTE = -1100 ppm/K

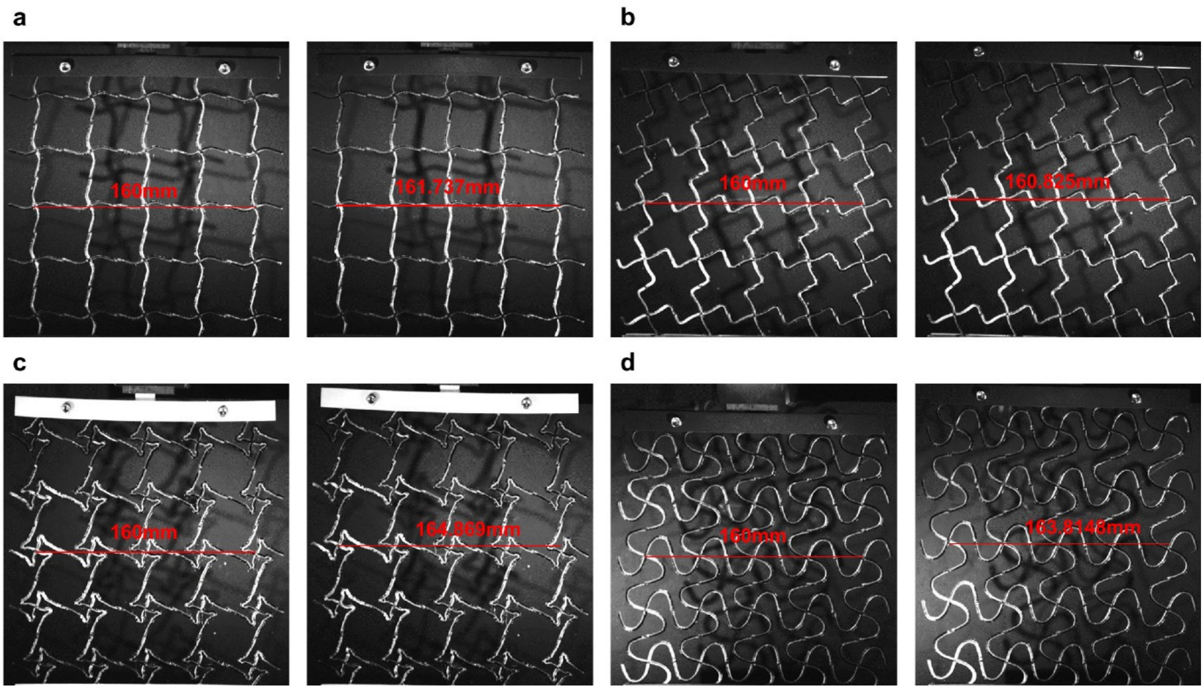

Fig. S9 PR experiment result (a) inverse design target PR = -0.4 (b) inverse design target PR = -0.1 (c) inverse design target PR = -0.6 (d) inverse design target PR = -0.2

7. Programmable thermal deformation

1	2	3	4	5	5	4	3	2	1
2	2	3	4	5	5	4	3	2	2
3	3	3	4	5	5	4	3	3	3
4	4	4	4	5	5	4	4	4	4
5	5	5	5	5	5	5	5	5	5
5	5	5	5	5	5	5	5	5	5
4	4	4	4	5	5	4	4	4	4
3	3	3	4	5	5	4	3	3	3
2	2	3	4	5	5	4	3	2	2
1	2	3	4	5	5	4	3	2	1

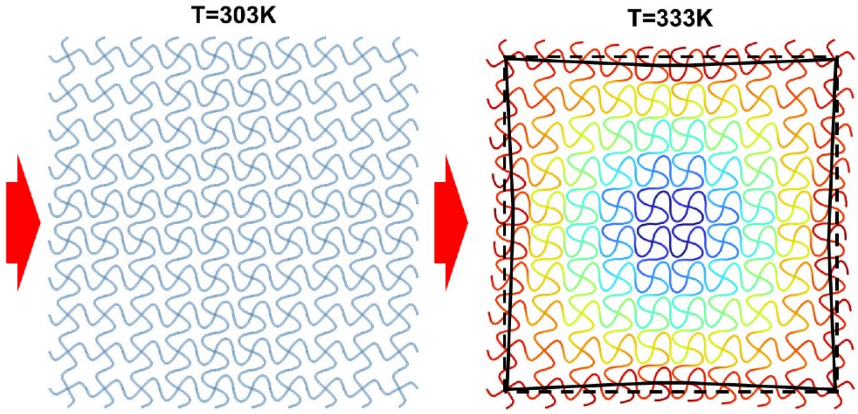

Fig. S10 Concave square thermal deformation mode

Reference

1. Y. Bai, C. Liu, Y. Li, J. Li, L. Qiao, J. Zhou and Y. Bai, *ACS applied materials & interfaces*, 2022, **14**, 35905-35916.
2. R. Lakes, *Journal of materials science letters*, 1996, **15**, 475-477.